Mixing system design for the Tati Activox® autoclave

by M. Nicolle*, G. Nel†, T. Plikas‡, U. Shah‡, L. Zunti‡, M. Bellino*, and
H.J.H. Pieterse§

Synopsis

The Tati Activox® Project will be the first full-scale implementation of the patented Activox® process (The Tati Activox® project was deferred in 2008. Please refer to the Norilsk Nickel press issue on the topic for more info). The process was developed by Norilsk Process Technology and has been tested on Tati mine sulphide concentrates in laboratory, pilot and demonstration plant scales and demonstrated its viability. There are inherent risks to the final scale-up of the process from the demo plant and one of them will be investigated in this paper.

Compartment 1 is designed to leach approximately 77% of the total nickel leached. For this reason agitation requirements in the first compartment of the autoclave are reviewed. An attempt is made to minimize the process and mechanical risks associated in achieving oxygen mass transfer into the slurry solution. The agitator powers for oxygen mass transfer are calculated using empirical correlations and compared to demonstration plant testwork. The resulting gassed power per unit volume (P/V) is higher than most commercial autoclaves and raises uncertainty on the viability of using such high unit power inputs. Additionally, there is concern about the ability of the autoclave shell to withstand and support the higher loading of large agitators. An alternative solution to designing for the increased P/V is assessed in which the number of compartments within the autoclave is reduced from 5 to 4 by removing the compartment wall separating compartments 1 and 2. This results in an enlarged first compartment containing 3 agitators instead of 2. Therefore the compartment 1 oxygen demand is supplied through 3 agitators, which lowers the P/V per agitator.

The reduction in the number of autoclave compartments raises the potential for short-circuiting the mean flow pattern by slurry particles. Short-circuiting and low velocity zones could result in a lower recovery of metal and localized hot spots, respectively. A computational fluid dynamic (CFD) analysis was conducted to quantify these concerns and also to evaluate further design considerations. The results indicate that the proposed design change to 4 compartments affects short-circuiting. The impact of increased short-circuiting on the overall autoclave recoveries is not quantified, however; it is expected to be negligible based on testwork done in the Tati Demonstration Plant and similar modifications made to another operating autoclave. The CFD analysis also suggests that there will be no low velocity zones within the compartment.

Introduction

Tati Nickel base metals refinery makes use of the patented Activox® process and will be the first full-scale commercial implementation. The ultra fine grinding (UFG) and autoclave pressure leach process conditions are the heart of the Activox® patent. The hydrometallurgical process has environmental and financial benefits over a pyrometallurigcal process in that it does not produce sulphur dioxide or acid as a by-product. The hydrometallurgical base metal refinery is designed to produce 25000 tpa nickel, 22000 tpa copper and 639 tpa cobalt as cobalt carbonate.

In the first phase of project implementation, process verification was completed during which the bankable feasibility study (BFS) design was assessed. Compartment one is designed to leach approximately 77% of the total nickel mass leached across the autoclave, as determined by the Tati Demonstration Plant campaigns. As a high portion of the leach reaction occurs in compartment one, significant attention was given to the compartment design. One particular area of review was the BFS basis for the oxygen mass transfer and dispersion within the autoclave's first compartment. The following sections of the paper outline the testwork completed and methods used to evaluate the mixer design in compartment 1 of the autoclave. This resulted in a design that was subjected to CFD modelling and analysis. The results of this analysis are used to validate aspects of the final autoclave design.

Process overview

The concentrate is repulped with copper raffinate and fed via attrition scrubbers to a UFG mill circuit. The mill circuit consists of primary and secondary mills in series, which

---

* *Hatch Africa (Pty) Ltd, South Africa.*
† *Norilsk Nickel Africa (Pty) Ltd, South Africa.*
‡ *Hatch (Pty) Ltd, Ontario, Canada.*
§ *Pieterse Consulting Inc., Arizona, USA.*

© *The Southern African Institute of Mining and Metallurgy, 2009. SA ISSN 0038–223X/3.00 + 0.00. This paper was first published in the proceedings of,* Hydrometallurgy 2008, *6th International Symposium, 17–20 August 2008, Phoenix Arizona.*

produce a finely ground concentrate. The size reduction significantly increases the surface area for the oxidation reactions to occur in the Activox® autoclave. Milled slurry is fed into 2 parallel Activox® autoclaves where the sulphide concentrate is oxidized. The autoclave operating temperature, pressure and chloride catalyst concentration result in the formation of favourable chemical species for handling downstream. Copper, cobalt and nickel are leached from the concentrate as sulphates in solution while elemental sulphur is formed as a by-product. Elemental sulphur, a solid, allows more cost-effective processing than sulphate ions, which would require neutralization before removal from the circuit. The oxidation of concentrate is exothermic and requires careful temperature control. Temperature is maintained by direct quenching and a flash recycle. Due to the moderate operating temperatures in the leach vessels, the flash cooling and flash discharge systems are operated at a vacuum to increase the heat removal. The flash vent gases report to a condenser where cooled water condenses vapour from the vent gases. Non-condensables and the remaining water vapour is drawn by a vacuum pump and discharged into a Venturi scrubber, which removes residual solids and entrained droplets, prior to discharge to the atmosphere.

The leach discharge slurry is cooled in slurry cooling towers after which it reports to the solid-liquid separation area where the leach residue solids are washed with recycled process water. The washed leach solids are then pumped to the platinum group elements (PGE) flotation circuit. The solution is clarified prior to solvent extraction, electrowinning and precipitation to produce nickel cathode, copper cathode and cobalt carbonate.

Basis for mixing system design

The Activox® autoclave mixing system design is based on the process conditions outlined in Table I.

Design development

The autoclave mixing system serves two purposes: firstly it creates an homogenous environment for the leach reactions to occur in by suspending the solids in the slurry, and secondly to replenish oxygen in solution as it reacts and oxidizes the ore. Gaseous oxygen is fed to each autoclave compartment through nozzles located under the agitator shafts and as such at the localized point in the autoclave with the highest shear. This maximizes oxygen mass transfer into the slurry solution whereafter it reacts with the sulphide ore according to the leach reactions.

Empirical correlation for the P/V

The agitation duty requirement in the first compartment is the greatest as the reactions in this compartment have the greatest oxygen demand. The stoichiometric mass of oxygen transferred into solution in compartment 1 is therefore critical to the leaching efficiency of the process. The transfer rate of oxygen to solution is known as the oxygen mass transfer rate (OTR) and is given in kg/m³/h. The OTR is a function of the mass transfer coefficient (k_L), the interfacial area (a), oxygen solubility in the slurry solution ($C_{O_2\text{-solution}}$) and the actual concentration of dissolved oxygen in solution (C). This relationship is shown in Equation [1].

$$OTR = k_L a\left(C_{O_2-solution} - C\right) \qquad [1]$$

The dissolved oxygen concentration C cannot be negative and the leach reaction extents are not controlled (the leach reactions are mass transfer limited when $C = 0$). Therefore, C must be greater than zero ($C > 0$) to achieve the required mass transfer. As the actual concentration of oxygen in the slurry solution cannot be greater than ($C_{O_2\text{-solution}}$), C is expressed as a percentage of ($C_{O_2\text{-solution}}$) in Equation [2].

$$C = \alpha C_{O_2-solution} \qquad [2]$$

From test work (which gives values for O_2 gassing rate and O_2 utilization) it is possible to determine the OTR per agitator using Equation [3]:

$$OTR = \frac{\left(O_{2-gassing\_rate}\right)\left(O_{2-utilization}\right)}{Liquid\_volume} \qquad [3]$$

where $O_{2\text{-gassing rate}}$ = 12 423/number of agitators in compartment 1 [kg/h]

$O_{2\text{-utlization}}$ = 0.90

Liquid volume = Slurry volume (1 – volume fraction of solids in slurry).

Table I

Process conditions in autoclave compartment one

Parameter	Value	Unit
Normal operating temperature	105	°C
Normal operating pressure	11	bar (a)
Oxygen (O_2) partial pressure	9.8	bar (a)
Compartment 1 nickel mass recovery	77	%
Stoichiometric O_2 required in the first compartment	11181	kg/h
O_2 gassing rate—total required in first compartment	12423	kg/h
O_2 utilization	90	%
Solids weight percent	35	% wt/wt
Solids specific gravity	2859	kg/m³
Liquor specific gravity	1304	kg/m³
Solids volume percent	19.7	%
Slurry volume C1A (BFS compartment 1, autoclave agitator 1)	51.8	m³
Slurry volume C1B (BFS compartment 1, autoclave agitator 2)	44.7	m³
Slurry volume C2C (BFS compartment 2, autoclave agitator 3)	42.7	m³

In order to calculate the mass transfer coefficient using Equation [1] the solubility of oxygen in slurry solution ($C_{O2\text{-}solution}$) must first be determined. ($C_{O2\text{-}solution}$) is lower than the solubility of oxygen in pure water ($C_{O2\text{-}water}$) due to the presence of dissolved salts. The relationship for ($C_{O2\text{-}water}$) is shown in Equation [4] (Tromans 1998).

$$C_{O_2-water} = p_{O_2}\left(\frac{1}{H}\right) \qquad [4]$$

where H = Henry's coefficient [kg.atm.mol^{-1}]
p_O = Partial pressure of oxygen gas [atm]
$C_{O2\text{-}water}$ = Molal concentration of dissolved oxygen in water [mol O_2. kg water^{-1}]

Henry's coefficient is calculated from the relationship given in Equation [5].

$$\left(\frac{1}{H}\right) = \exp\left(\frac{0.046T^2 + 203.357T\ln\left(\frac{T}{298}\right) - (299.378 + 0.092T)(T-298) - 20.59\cdot 10^3}{8.3144T}\right) \qquad [5]$$

Where T = temperature in K.

At the process temperature of 105°C (378K)

$$\left(\frac{1}{H}\right) = 0.00078515\frac{mol}{kg\cdot atm}$$

To convert to units of $\frac{g}{L\cdot atm}$ the formula must be multiplied by the density of water and the molecular weight of oxygen:

$$\left(\frac{1}{H}\right) = 0.00078515\frac{mol}{kg\cdot atm}\cdot\frac{1kg\,32g}{L\,mol} = 0.0251\frac{g}{L\cdot atm}$$

The oxygen solubility is lowered due to the presence of dissolved salts (mainly nickel, copper and cobalt sulphate) by a derating factor, φ (Tromans 1998). The relationship between solution oxygen solubility and water oxygen solubility is shown in Equation [6].

$$C_{O_2-solution} = \varphi\cdot C_{O_2-water} \qquad [6]$$

The value of φ from Equation [6] is determined (using Figure 6 in Tromans 1998) with the expected molal concentration of nickel, copper and cobalt sulphate in the solution (2.047 mol/kg). φ is approximately 0.70 to 0.75. It is now possible to calculate C from Equation [2] as α varies between 0.2 and 0.3 according to industry norms. A value of 0.3 was used in this case and this assumption was validated at a later stage through testwork. It is anticipated that high actual concentrations of oxygen in solution (C) are unlikely due to the high sulphide concentration in the Tati concentrate slurry. With C known it is possible to calculate k_La from Equation [1], and so from Equation [7] below the gassed power per unit volume (P/V). The P/V required is calculated using the empirical Equation [7] (based on a recommendation made by Pieterse 2004) and adjusted using data the authors subsequently obtained from several commercial sized autoclaves.

$$k_La = 381.397\left(\frac{P}{V}\right)^{0.76} \qquad [7]$$

where P/V = gassed power per unit volume in kW.m^{-3}
And k_La = the mass transfer coefficient in h^{-1}

P/V calculation for two agitators in compartment 1

The resulting power demand (3.89 kW/m³ – 4.73 kW/m³) on the agitators is very high in comparison to commercial autoclaves. This high power demand results in a very large agitator and raises concerns about the ability for the autoclave shell design to support the large weight and forces without the need for significant localized strengthening.

By removing the weir wall separating compartment 1 from 2 the new compartment 1 will have 3 agitators under which the required oxygen can be added. This configuration is assessed in the same way as the scenario with 2 agitators in compartment 1. (Table II.)

P/V calculation for three agitators in compartment 1

Table III summarizes the empirical calculation outlined in the section 'Empirical correlation for the P/V' of this paper. The same conditions as Table II were used with the exception that the oxygen demand was split over 3 agitators and not 2.

The reduction in oxygen demand per agitator and subsequent reduced P/V (from between 3.89 kW/m³–4.73 kW/m³ to between 2.28 kW/m³ to 2.94 kW/m³) reduces concern about the agitator support on the autoclave shell as there are a limited number of commercial autoclaves operating under similar agitator duties and supports to those proposed for this application.

Testwork in Tati demonstration plant

Testwork was carried out on the Tati demonstration plant in Botswana in order to further clarify the agitation requirements of the autoclave. These test results were compared to the empirical results to develop confidence in the proposed commercial design. The results of the testwork are summarized in Table IV. The same conditions as Table II were used with the exceptions listed below. Most importantly the oxygen demand is lower than the commercial plant.

By comparing the average measured P/V from the testwork and that calculated using Equation [7] in Table IV it

Table II

A summary of the empirical calculation as applied to 2 agitators in compartment 1

O_2 gassing rate per agitator	6212 kg/h
Weight per cent solids	35% wt/wt
Specific gravity solids	2859 kg/m³
Specific gravity liquor	1304 kg/m³
Volume per cent solids	19.7% vol./vol.
Slurry volume—C1A	51.82 m³
Slurry volume—C1B	44.65 m³
Oxygen solubility in water—Equation [4]	0.2430 kg/m³
Derating factor—Equation [6]	0.735
O_2 solubility in solution—Equation [6]	0.1786 kg/m³
Dissolved O_2 as % of soluble O_2 in solution	30%
Dissolved O_2 concentration in solution—Equation [2]	0.0536 kg/m³
Oxygen transfer rate in C1A—Equation [3]	134 kg/h.m³
Oxygen transfer rate in C1B—Equation [3]	155 kg/h.m³
k_La in C1A—Equation [1]	1069 h^{-1}
k_La in C1B—Equation [1]	1241 h^{-1}
P/V required in C1A [7]	3.89 kW/m³
P/V required in C1B [7]	4.73 kW/m³

Table III

A summary of the empirical calculation as applied to 3 agitators in compartment 1

O$_2$ gassing rate per agitator	4141 kg/h
Oxygen solubility in water—Equation [4]	0.2430 kg/m^3
O$_2$ solubility in solution—Equation [6]	0.1786 kg/m^3
Dissolved O$_2$ concentration in solution—Equation [2]	0.0536 kg/m^3
Oxygen transfer rate in C1A—Equation [3]	89 kg/h.m^3
Oxygen transfer rate in C1B—Equation [3]	103 kg/h.m^3
Oxygen transfer rate in C1C—Equation [3]	108 kg/h.m^3
k_La in C1A—equation [1]	713 h^{-1}
k_La in C1B—equation [1]	827 h^{-1}
k_La in C1C—equation [1]	865 h^{-1}
P/V required in C1A [7]	2.28 kW/m^3
P/V required in C1B [7]	2.77 kW/m^3
P/V required in C1C [7]	2.94 kW/m^3

Table IV

A summary of the empirical calculation as applied to 8th March 2007 testwork results

O$_2$ gassing rate per agitator	36 kg/h
Weight percent solids	35% wt/wt
Specific gravity solids	2859 kg/m^3
Specific gravity liquor	1200 kg/m^3
Volume percent solids	18.4% vol./vol.
Slurry volume—C1A	0.64 m^3
Slurry volume—C1B	0.58 m^3
Oxygen solubility in water—Equation [4]	0.2430 kg/m^3
O$_2$ solubility in solution—Equation [6]	0.1786 kg/m^3
Dissolved O$_2$ concentration in solution—Equation [2]	0.0536 kg/m^3
Oxygen transfer rate in C1A—Equation [3]	62 kg/h.m^3
Oxygen transfer rate in C1B—Equation [3]	69 kg/h.m^3
k_La in C1A—Equation [1]	497 h^{-1}
k_La in C1B—Equation [1]	552 h^{-1}
P/V required in C1A [7]	1.42 kW/m^3
P/V required in C1B [7]	1.63 kW/m^3
Average P/V measured in C1A	2.64 kW/m^3
Average P/V measured in C1B	2.93 kW/m^3

Table V

Demo plant P/V with OTR in the region of 89–108 kg/m^{3}h

O$_2$ gassing rate per agitator	53.3 kg/h
Oxygen solubility in water—Equation [4]	0.2430 kg/m^3
O$_2$ solubility in solution—Equation [6]	0.1786 kg/m^3
Dissolved O$_2$ concentration in solution—Equation [2]	0.0536 kg/m^3
Oxygen transfer rate in C1A—Equation [3]	92 kg/h.m^3
Oxygen transfer rate in C1B—Equation [3]	102 kg/h.m^3
k_La in C1A—Equation [1]	739 h^{-1}
k_La in C1B—Equation [1]	819 h^{-1}
P/V required in C1A [7]	2.39 kW/m^3
P/V required in C1B [7]	2.74 kW/m^3

is possible that during the testwork either the agitator power was higher than the power required for oxygen mass transfer or that too low a value for α (from Equation [2], $\alpha = 0.3$) had been assumed. It was suspected that the agitator power was higher than the power required for oxygen mass transfer. This suspicion was confirmed by additional tests (summarized in Figure 1 in which the P/V was reduced but no appreciable change in Ni metal recovery was recorded until the P/V dropped below well 1.4 kW/m^3. The P/V for compartment 1A, as calculated in Table IV and based on the assumption that a = 0.3, is 1.42 kW/m^3. Hence the original assumption that a = 0.3 is validated.

The demo plant OTR is 62–69 kg/m^{3}h while the commercial plant's design OTR is 89–108 kg/m^{3}h. The commercial design takes into account the potential for an ore with a high sulphur content that will require additional oxygen per unit mass of feed solids to leach. In order to compare the same oxygen inputs the Tati demonstration plant conditions are recalculated in Table V to indicate what the P/V would be if the OTR were in the region of 89–108 kg/m^{3}h. The resulting P/V is between 2.39–2.74kW/m^3, which is similar to the commercial plant requirements in Table III. The same conditions as Table IV were used with the exception that the OTR was increased to what the commercial plants design will be.

It should be noted that the Tati demonstration plant oxygen transfer rates (OTR) are only a guideline and cannot be scaled up linearly.

Design considerations

Agitator design

Table VI shows the proposed design of the agitator to meet the mass transfer requirements outlined in Table III.

A custom 8-bladed Rushton turbine with increased blade height connected to a 186 kW variable speed drive motor was selected. Increasing the blade height is a common means of increasing the power number of a Rushton turbine. The recommended design shaft speed is 92 rpm, which produces a gassed power input of 129 kW (69% of motor load) per agitator and a volume averaged P/V of 2.8 kW/m^3 in the compartment. The design shaft speed results in an impeller tip speed of 6.5 m/s, which is below the design maximum of 7 m/s, reducing impeller blade erosion. At the maximum motor load (~85%) the volume averaged power per unit volume is 3.4 kW/m^3.

From Table VI the comparative P/Vs indicate that the proposed 3 agitator first compartment arrangement adequately provides the required P/V range obtained from empirical calculations.

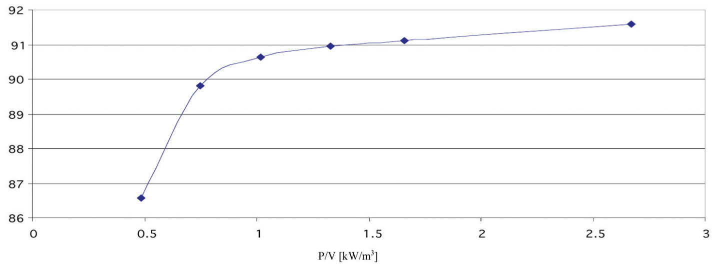

Figure 1—Effects of P/V on nickel recovery recorded in theTati demonstration plant

Table VI

P/V from the proposed design

Agitator	P/V required Equation [7]	P/V measured during 8 March 2007 testwork	P/V at 69% of motor capacity	P/V at 85% of motor capacity	Unit
Compartment 1 A	2.28	2.64	2.49	3.05	kW/m³
Compartment 1 B	2.77	2.93	2.89	3.54	kW/m³
Compartment 2 C	2.94		3.02	3.70	kW/m³

Table VII

P/V sensitivity analysis on assumed a values

α	$C_{O_2\text{-solution}}\left(\frac{kg}{m^3}\right)$	$C\left(\frac{kg}{m^3}\right)$	$k_La\ (h^{-1})$	Required $\frac{P}{V}\left(\frac{kW}{m^3}\right)$
0	0.1822	0	C1A: 49 C1B: 579 C2C: 605	C1A: 1.43 C1B: 1.73 C2C: 1.84
0.1	0.1822	0.0179	C1A: 554 C1B: 643 C2C: 673	C1A: 1.64 C1B: 1.99 C2C: 2.11
0.2	0.1822	0.0357	C1A: 624 C1B: 724 C2C: 757	C1A: 1.91 C1B: 2.33 C2C: 2.47
0.3	0.1822	0.0536	C1A: 713 C1B: 827 C2C: 865	C1A: 2.28 C1B: 2.77 C2C: 2.94
0.4	0.1822	0.0714	C1A: 831 C1B: 965 C2C: 1009	C1A: 2.79 C1B: 3.40 C2C: 3.60
0.5	0.1822	0.0893	C1A: 998 C1B: 1158 C2C: 1211	C1A: 3.55 C1B: 4.32 C2C: 4.58

Agitator design sensitivity

The sensitivity of the power per unit volume to the assumed value of a for the proposed commercial autoclave is summarized in Table VII.

Table VII indicates the high sensitivity that the required P/V has to the assumed value of a. For this reason the additional flexibility offered by the proposed agitators is important. Calculations indicate that at the maximum motor load (~85%) $\alpha = 0.42$ and provides an additional design margin on agitator power.

Short-circuiting

By reducing the number of compartments from 5 to 4 the potential for slurry particles to short-circuit in the autoclave and exit unreacted is increased. This would lead to lower metal recoveries. A factor that will help minimize the affect of short-circuiting on overall recovery is the small contribution of compartment 5 to the overall recovery. This is supported by data collected during test runs on the pilot plant in which compartment 5 increased the overall recovery of nickel, copper and cobalt by an average of 0.3%, 0.9% and 0.2% respectively.

Short circuiting was analysed by performing a CFD analysis and is outlined in the next section. This analysis provided insight into the 3 agitator configuration in sufficient detail to determine if the proposed arrangement will experience short-circuiting.

Objectives of CFD modelling

A CFD model was used to evaluate the following design objectives:

- Determine overall mixing and flow patterns in compartment 1 to determine the effect on process performance
- Determine the optimum impeller and baffle configuration that maximizes back mixing in compartment 1 while minimizing swirling flows beneath the impeller that lead to vessel lining wear
- Determine impeller rotation direction
- Determine if the required slurry particle residence time in compartment 1 is achieved given the large recirculation flow of slurry through the flash cooling and autoclave feed system.

CFD simulation results

A three dimensional CFD model of the first compartment in the autoclave was constructed to its actual dimensions. Figure 2 shows the model. The model was set up with the following boundary conditions (see Figure 2 for location of each):

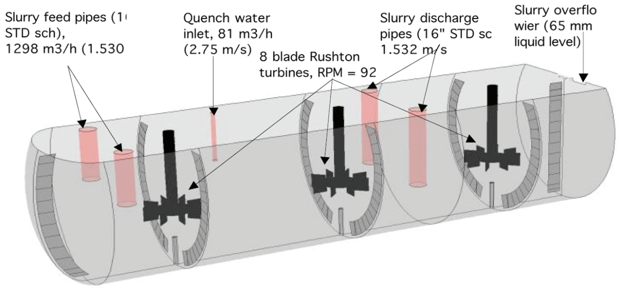

Figure 2—Geometric model of autoclave first compartment illustrating major conditions

- Slurry feed inlet—velocity inlet boundary
- The overflow from the weir—pressure outlet boundary
- The slurry free surface—zero shear (slip boundary)
- Vessel walls—no slip boundary.

Agitator rotation direction

The mixing was analysed with each of the agitators operating at a 92 rpm. Two different cases were studied.

1. All three agitators rotating in the same direction
2. Middle agitator rotating in the opposite direction.

Figure 3 shows the velocity profile of the slurry on a horizontal plane 1.863 m from the slurry free surface. The following observations were made:

- There is weak interaction between the flow from adjacent agitators and the overall flow pattern was found to be similar for both cases.
- The dotted lines represent the net slurry flow from the feed end to the discharge end. It indicates a different flow pattern for the net slurry given the agitator rotation direction. However, it was observed that the net slurry flow path length was approximately the same for both cases. The residence time distribution (RTD) of the slurry explains this quantitatively in a later section.

Figure 4 shows that this agitator and baffle configuration produces two distinct flow loops – one in the upper half of the vessel and one in the lower half. This is required for suspension of solids and effective top to bottom blending of solids with dissolved oxygen.

Figure 5 and Figure 6 show the velocity profile on a vertical plane. Similar flow patterns were observed for both cases (same rotation and middle agitator—reverse rotation). It was also observed that the slurry flow to the discharge dip-pipes is predominantly from the middle agitator. The flash discharge pipes are positioned at the location shown to allow a compartment wall to be inserted between the second and third agitator. A previous CFD analysis showed this as the optimum location for the dip-pipes for an autoclave with two agitators in C1 and therefore provides the option to revert to a two agitator compartment if desired.

Swirling flow beneath the impeller is unavoidable as angular momentum is imparted to the slurry by the rotating impeller. Larger solids caught up in this swirling vortex can cause erosion of the vessel lining underneath the impeller. Therefore, it is important to minimize the magnitude of such swirling velocities. Extending the baffles closer to the bottom can minimize the swirling velocity significantly. The final baffle configuration is shown in Figure 2. Note that extending

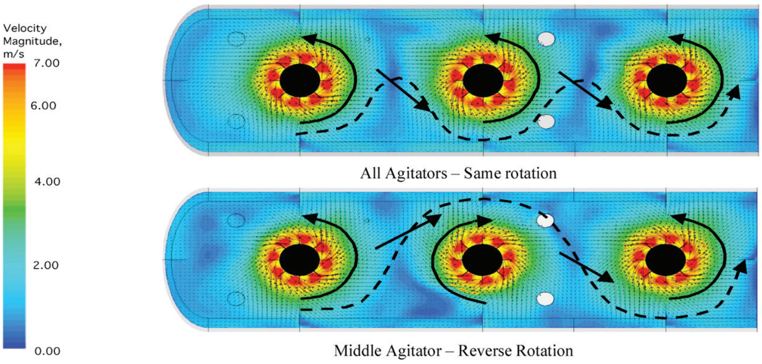

All Agitators – Same rotation

Middle Agitator – Reverse Rotation

Figure 3—Slurry velocity profile, coloured by velocity magnitude (m/s) on a horizontal plane across impellers. Lines represent the net slurry flow direction

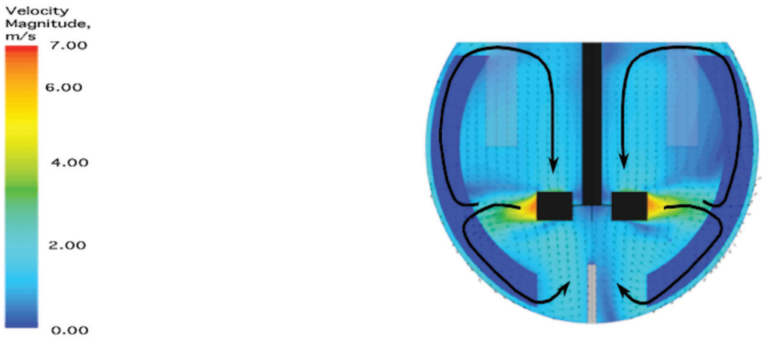

Figure 4—Slurry velocity profile, coloured by velocity magnitude (m/s) on a vertical plane across impellers. Lines represent the net slurry flow direction

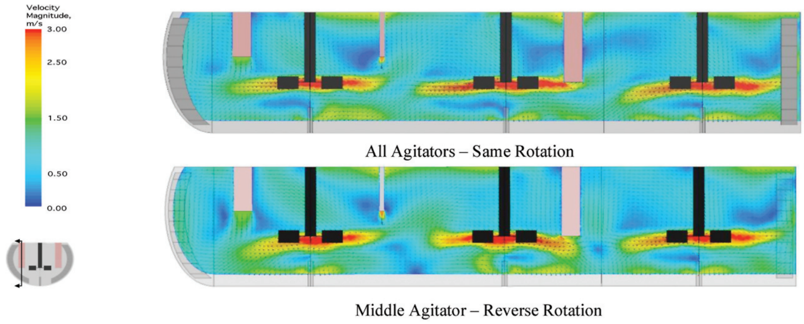

All Agitators – Same Rotation

Middle Agitator – Reverse Rotation

Figure 5—Velocity profile, on a vertical plane cutting through the left-side (looking downstream) feed and discharge pipes illustrating the slurry flow pattern

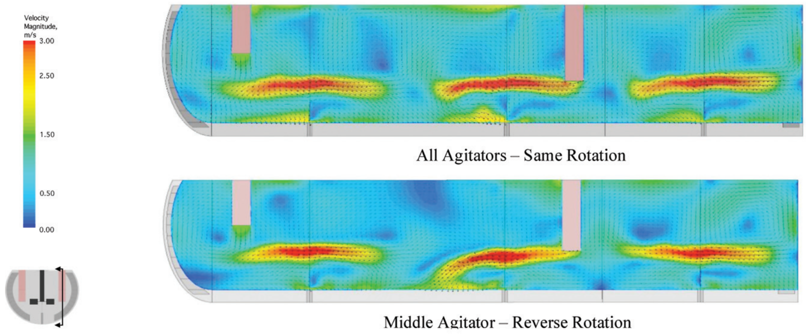

All Agitators – Same Rotation

Middle Agitator – Reverse Rotation

Figure 6—Velocity profile, coloured by velocity magnitude (m/s) on a vertical plane cutting through the right-side (looking downstream) feed and discharge pipes illustrating the slurry flow pattern

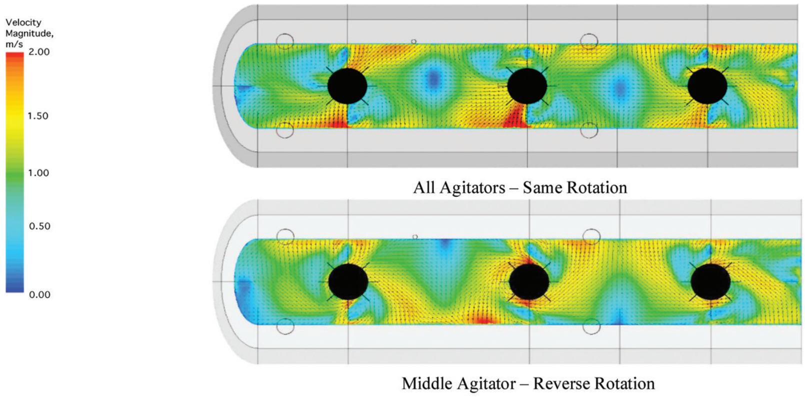

All Agitators – Same Rotation

Middle Agitator – Reverse Rotation

Figure 7—Velocity profile, coloured by velocity magnitude (m/s) on a horizontal plane at 0.3 m off-bottom distance and cutting along the compartment illustrating the swirl velocity magnitudes

the baffles right to the bottom of the vessel, breaks the single swirling vortex into 2 or more smaller vortices on either side of the baffle. These smaller vortices can actually rotate at a higher velocity than the single swirling vortex beneath the impeller accelerating the erosion rate of the vessel lining over a smaller, localized region.

Figure 7 shows the velocity profile on a horizontal plane at an off-bottom distance of 0.3 m illustrating swirling velocity magnitudes on a plane underneath the impellers. A maximum velocity magnitude of 2 m/s was observed for both cases. It must be noted that the velocities should not be minimized to an extent that can allow solids settling, and therefore movement of solids along the vessel bottom is required to avoid solids packing. For the Tati Activox® process, solids suspension does not appear to be a concern due to the very small particle sizes of solids in the slurry feed (P80=10 μm).

The general flow field results indicate that the slurry flow inside the first compartment is well mixed and no low velocity regions are observed that could otherwise allow the formation of hot spots. The mixing is quantitatively described by the turnover rate of slurry volume for the agitator discharge flow. Turnover rates greater than 3 are required for medium to violent agitation (Bowen 1985). The CFD model predicts a flow rate of 20 000 m^3/h is generated by a single impeller corresponding to 7.2 turnovers per minute.

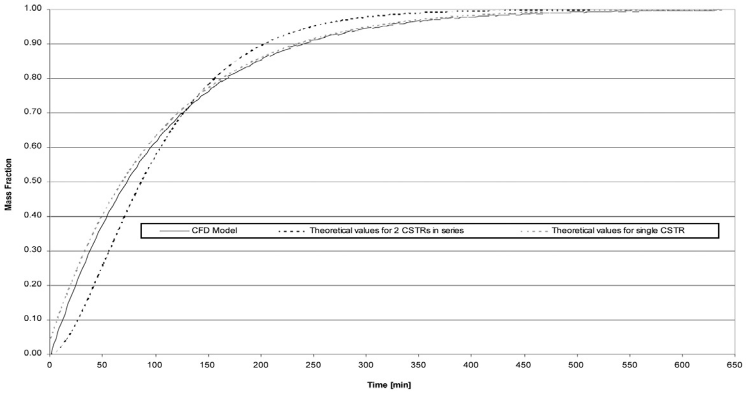

Figure 8—Residence time distribution comparison

Residence time distribution (RTD)

The residence time distribution of the slurry in the compartment can also be used to evaluate the mixing performance and its subsequent effect on recovery. A tracer analysis was performed to determine the residence time distribution. Mass-less tracers, which follow the slurry flow closely, were injected into the compartment through the feed inlets and tracked to determine their residence time. The slurry exiting through the discharge pipe is recycled back to the front of the compartment after flash cooling. Thus, fresh slurry fed to the first compartment will flow through a number of recycles before it overflows to the second compartment.

Figure 8 shows the RTD results for the tracer analysis, single continuous stirred reactor (CSTR) and for 2 CSTRs in series (calculated from Davis 2002). The RTD for two CSTRs in series represents the autoclave with the additional weir wall in place. The CFD model predicts an RTD similar to what would be expected from a single CSTR. When comparing the CFD model and the 2 CSTRs RTD the potential for short-circuiting is likely.

The impact of the increased material short-circuiting on the overall autoclave recoveries still needs to be quantified; however, it is expected to be negligible based on testwork done in the Tati demonstration plant and similar modifications done on other operating autoclaves.

Conclusion

Based on all of the calculations and CFD analysis, the following conclusions were reached:

- The general flow field results indicate that the flow inside compartment 1 is well mixed and no distinct low velocity regions are seen that may form ‘hot spots’.
- The impact of increased short circuiting on the overall autoclave recoveries still needs to be quantified, however; it is expected to be negligible based on testwork done in the Tati demonstration plant and similar modifications made on other operating autoclaves.
- Due to the small particle sizes of the solids in the incoming slurry feed (P80=10 μm), solids suspension is not a concern, and it is expected that solids will be uniformly suspended to the full liquid height of the autoclave.
- Very good mixing between solids and dissolved oxygen is expected, leading to a uniform leach reaction extent and process temperature throughout the vessel volume.
- A baffle off-bottom clearance of 0.14 D was found to be optimum to minimize the swirling velocity near the tank bottom.
- There is weak interaction between the discharge flow from adjacent agitators for the given operating condition and the overall flow patterns are uninfluenced by the relative rotational direction of adjacent agitators.
- Different flow patterns for the net slurry flow from the feed end to the discharge end was observed for the two cases: (1) all agitators—same rotation direction and, (2) middle agitator—reverse rotation. However, it was observed that the net slurry flow path length is approximately the same for both the cases.

Acknowledgements

The authors acknowledge that this paper was originally published as part of the proceedings of Hydrometallurgy 2008—6th International Symposium honoring Robert Shoemaker, August 17–20, 2008, Phoenix, AZ.

The authors would like to thank the management of Norilsk Nickel Africa, Norilsk Process Technology and Hatch for their encouragement and permission to publish this paper.

References

Tromans, D. Temperature and Pressure Dependant Solubility of Oxygen in Water: A Thermodynamic Analysis. *Hydrometallurgy*, vol. 48, 1998. pp. 324–342.

Tromans, D. Oxygen Solubility Modeling in Inorganic Solutions: Concentration, Temperature and Pressure Effects. *Hydrometallurgy*, vol. 50, 1998. pp. 279–296.

Pieterse, H. Oxidation Autoclave Agitation Review. *Pressure Hydrometallurgy 2004, 34th Annual Hydrometallurgy Meeting*, Banff, Alberta, Canada. 2004.

Bowen, R.L. Agitation Intensity: Key to Scaling Up Flow-Sensitive Liquid Systems. *Chemical Engineering*, March 18, 1985.

Davis, M.E. and Davis, R.J. *Fundamentals of Chemical Reaction Engineering*. Mcgraw-Hill Chemical Engineering Series, International Edition, July 2002.

◆